

Low temperature physics at room temperature in water: Charge inversion in chemical and biological systems

A.Yu. Grosberg, T.T. Nguyen, and B.I. Shklovskii

Department of Physics, University of Minnesota, 116 Church Street SE, Minneapolis, Minnesota 55455

We review recent advances in physics of strongly interacting charged systems functioning in water at room temperature. We concentrate on the phenomena which go beyond the framework of mean field theories, whether linear Debye-Hückel or non-linear Poisson-Boltzmann. We place major emphasis on charge inversion - a recently discovered counterintuitive phenomenon in which a strongly charged particle, called macroion, binds so many counterions that its net charge changes sign. We discuss the universal theory of charge inversion based on the idea of strongly correlated liquid of adsorbed counterions, similar to a Wigner crystal. This theory has vast array of applications, particularly in biology and chemistry; for example, DNA double helix in presence of positive multivalent ions acquires net positive charge and drifts as a positive particle in electrophoresis. We discuss also the experimental evidence of charge inversion and its analogies in physics.

CONTENTS

| | |
|---|----|
| I. Introduction | 1 |
| II. Historical remarks: Mean field theories | 3 |
| III. Strongly correlated liquid of multivalent ions | 4 |
| IV. Correlation-induced charge inversion | 5 |
| V. Enhancement of charge inversion by monovalent salt | 6 |
| VI. Screening of a charged plane by polyelectrolytes | 7 |
| VII. Polyelectrolytes wrapping around charged particles | 8 |
| VIII. Multilayer adsorption | 9 |
| IX. Correlation induced attraction of like charges | 9 |
| X. Experimental evidence of charge inversion | 11 |
| XI. Apart from correlations, does anything else drive charge inversion? | 12 |
| XII. Charge inversion in a broader physics context | 13 |
| ACKNOWLEDGMENTS | 14 |
| References | 14 |

I. INTRODUCTION

Molecular biological machinery functions in water near the room temperature. For a physicist, this very limited temperature range contrasts unfavorably to the richness of low temperature physics, where one can change temperature and scan vastly different energy scales in orderly manner. In this article, we review the recently developed understanding of highly charged molecular systems in which Coulomb interactions are so strong that we are effectively in the realm of low temperature physics.

To be specific, imagine a problem in which one big ion, called *macroion*, is screened by much smaller but still multivalent ions with a large charge Ze each (e is the proton charge); for brevity, we call them Z -ions. A variety of macroions are of importance in chemistry and biology, ranging from the charged surface of mica or charged solid particles, to charged lipid membranes, colloids, DNA, actin, to cells and viruses. Multivalent metal ions, charged micelles, dendrimers, short or long

polyelectrolytes including DNA - to name but a few - can play the role of screening Z -ions.

The central idea of this article is that of *correlations*: due to strong interactions with the macroion surface and with each other, screening Z -ions do not position themselves randomly in three-dimensional space, but form a strongly correlated liquid on the surface of a macroion. Moreover, in terms of short range order this liquid reminds a Wigner crystal, as the cartoon in the Fig. 1 depicts. Because of central importance we shall use special abbreviation SCL for strongly correlated liquid of adsorbed Z -ions.

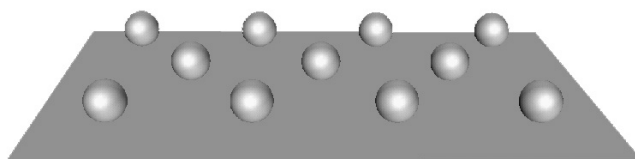


FIG. 1. Strongly correlated liquid (SCL) - almost a Wigner crystal - of Z -ions on the oppositely charged macroion surface.

Fig. 1 is characteristic in showing the degree to which we ignore the microscopic details. Although there are many complications, ranging from hydration to dielectric discontinuity to possible breakdown of continuum electrostatics at nanometer scale, we concentrate in this work on the simplified models. In real chemical and biological systems, other factors may be also at work, but our goal is to show that electrostatic correlations are always important when multivalent ions are involved in screening.

Depending on the system geometry and other circumstances, correlations between screening ions may appear very differently. To create some simple images in the reader's mind, it is useful to begin with a few examples. One example is the Fig. 1, which may be the surface of, e.g., a latex particle screened by some compact ions.

With a modest leap of imagination, we can pretend the same picture to represent a surface of DNA double helix screened by multivalent counterions, such as spermine with $Z = 4$ (Bloomfield, 1996). Here, we imagine DNA as a thick and long cylinder, diameter 2 nm and charge $-e$ per 1.7 nm along the cylinder, or, in other words, with a huge negative surface charge density $-0.9 e/\text{nm}^2$. We study correlations between point-like Z -ions in the Secs. III - V.

In another example, DNA molecules play the role of Z -ions screening the surface of a colloid particle. For very short DNA pieces we are back again to the Fig. 1, but longer DNA are spaghetti-like, and in this situation, correlations mean parallel arrangement, as we see in the Fig. 2. Theoretical treatment of this problem in the Sec. VI simplifies it as a system of parallel rods.

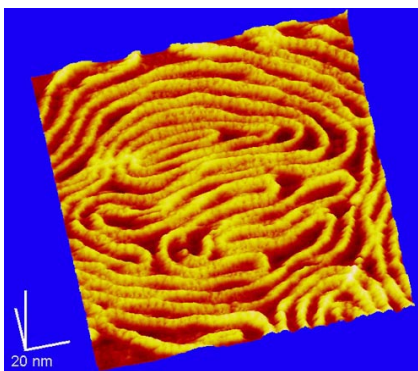


FIG. 2. DNA adsorbed on the positively charged surface, as seen in the atomic force microscopy image (Mou et al, 1995).

Electrostatic correlations are strong not only for artificial systems involving DNA, but also for the DNA in the cell (Aberts et al, 1994). In particular, to organize DNA in chromatin (in eukariotic cells), nature uses strongly positively charged proteins - histones. Higher levels of chromatin hierarchial structure can be disassembled, with some of the histones released, by elevated concentration of salt. The resulting most stable lower level structure is a bead-on-a-string necklace, as shown in the Fig. 3. It is called 10 nm fiber, because the beads, called nucleosomes, are about that big. Each nucleosome consists of a core particle, called octamer, with total charge about $+170e$. As shown in the inset in the Fig. 3, octamer is wrapped around by 1.8 turns of DNA, with charge $-292e$. Electrostatic interaction energy between DNA and histone octamer dwarfs bending energy of DNA. Strikingly, a simple theory discussed in the Sec. VII yields a similar structure, Fig. 4, based on purely electrostatic correlations in a simple model.

Correlated screening has also many more practical applications, ranging from the idea of manufacturing nanowires by attaching positive silver or gold colloids to DNA (Braun et al, 1998; Keren et al, 2001), to the technology of dressing of DNA with strongly positively charged mi-

cells, dendrimers, or liposomes (Radler et al, 1997; Evans et al, 2001) to deliver it into the cell for the purposes of gene therapy (Felgner, 1997).

We view these examples as convincing enough to engage in the study of electrostatic correlations between strongly charged screening Z -ions. Strong correlations manifest themselves in a number of ways and alter dramatically the whole picture of screening. In the familiar Debye theory, screening atmosphere somewhat reduces the effective value of charge as seen from a finite distance in the outside world. With strongly correlated ions, over-screening becomes possible, in which shielded macroion charge is seen from outside as having the inverted sign.

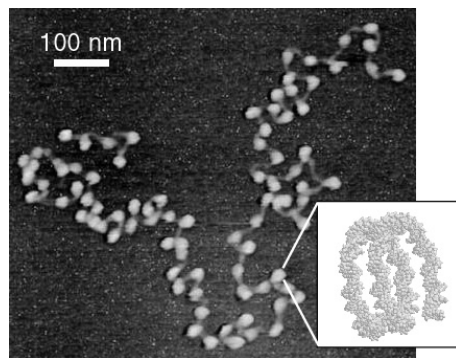


FIG. 3. Electron microscopy image of 10 nm chromatin fiber (Shao, 1999). The beads are nucleosomes. The structure of nucleosome is known to about 0.2 nm resolution (Luger et al, 1997), and the inset shows how DNA double helix is bent in the nucleosome. While overall shape of the fiber is perhaps due to the sample preparation procedure, the array of nucleosomes on the DNA is close to periodic, similar in this respect to the theoretical model shown in the Fig. 4.



FIG. 4. Self-assembled complex of a negative polyelectrolyte molecule and many positive spheres in a necklace-like structure. On the surface of a sphere, neighboring polyelectrolyte turns are correlated similar to rods in Fig. 7. At larger scale, charged spheres repel each other and form one-dimensional Wigner crystal along the polyelectrolyte molecule.

Such counterintuitive *charge inversion* is predicted to occur whenever screening ions are strongly charged. Furthermore, since they bind to macroion with energies well in excess of $k_B T$, the inverted net charge should be easily observable: it is the sign of the net charge that determines the direction of a macroion drift in a weak field electrophoresis. In essence, this theory predicts that at large enough concentration of Z -ions DNA drifts to the negative pole in an applied electric field. In particular, charge inversion should simplify DNA uptake by the cell

as needed for gene therapy, because cell membrane is negatively charged. This situation is generic and is expected in all systems where strongly charged ions participate in screening. Charge inversion, which can exceed hundred percent of the original macroion charge, turns out to be a natural manifestation of correlations between screening ions. In the recent years, the phenomenon of charge inversion attracted quite significant attention (Ennis et al, 1996; Wallin and Linse, 1996; Perel and Shklovskii, 1999; Shklovskii, 1999b; Mateescu et al, 1999; Park et al, 1999; Joanny, 1999; Sens and Gurovich, 1999; Netz and Joanny, 1999a; Netz and Joanny, 1999b; Wang et al, 1999; Nguyen et al, 2000a; Nguyen et al, 2000b; Messina et al, 2000; Nguyen and Shklovskii, 2001a; Chodanowski and Stoll, 2001; Nguyen and Shklovskii, 2001b; Dobrynin et al, 2001; Andelman and Joanny, 2000; Potemkin et al, 2001; Tanaka and Grosberg, 2001a; Nguyen et al, 2000.)

Another equally interesting manifestation of correlations is the possibility of attraction between like charged macroions mediated by Z -ions. This has implications in the large field of self-assembly of charged biological objects, ranging from RNA (Woodson, 2000; Pan et al, 1999) to virus heads (Gelbart et al, 2000). In Sec. IX, we show how this attraction of like charges competes with repulsion due to inverted charges, causing together reentrant condensation in the solutions of DNA or colloids.

In what follows, we re-examine the entire concept of screening to include correlations. Although this requires stepping beyond the mean field approximation, we shall start with some historical remarks which also serve to define the notations.

II. HISTORICAL REMARKS: MEAN FIELD THEORIES

The history of our subject is almost one century long. We don't plan to discuss it here in any depth, we shall only mention three key steps.

In the first step, Gouy (1910) and independently Chapman (1913) examined the double layer at an electrode surface, an intensely disputed subject at the time. Following Gouy and Chapman, let us consider a massive insulating macroion. To be specific, assume that its charge is negative, with surface density $-\sigma$. Assume further that the only counterions in the system are those dissociated from the surface. Since macroion is large, the problem of counterions distribution near the surface is one-dimensional, with both counterion concentration $N(x)$ and electrostatic potential $\phi(x)$ depending on the distance x from the surface. Gouy and Chapman addressed this problem by solving what we now call the non-linear mean field Poisson-Boltzmann equation:

$$\Delta\phi = -\frac{4\pi}{\epsilon}N_s eZ \exp\left[-eZ\frac{\phi(x) - \phi_s}{k_B T}\right]. \quad (1)$$

Here $\epsilon \approx 80$ is the dielectric constant of water, ϕ_s and N_s are the potential and counterion concentration at the surface. In Eq. (1), Poisson equation for the potential $\phi(x)$ is complemented by the assumption that ions determining charge density are self-consistently Boltzmann-distributed. One boundary condition $d\phi/dx|_{x=0} = 4\pi\sigma/\epsilon$ follows from the fact that the field vanishes on the other side of the boundary (as there is no electrolyte and no charges). The second condition is that concentration $N(x)$ must be normalized to σ/Ze ions per unit area. The exact solution of thus formulated Gouy-Chapman problem reads

$$N(x) = \frac{k_B T \epsilon / 2\pi e^2 Z^2}{(x + \lambda)^2}, \quad (2)$$

where λ is called Gouy-Chapman length, it is equal to

$$\lambda = k_B T \epsilon / 2\pi \sigma Z e. \quad (3)$$

The interpretation of Eq. (3) is interesting. If a Z -ion were to be alone next to the charged plane, it would "jump" in the surface field $2\pi\sigma/\epsilon$ at such a "height" λ at which its energy $2\pi\sigma Z e \lambda/\epsilon$ is about $k_B T$ - which leads to the correct answer Eq. (3). Other Z -ions cancel the field inside the macroion but double the field in the electrolyte at the macroion surface (see above the boundary condition at $x = 0$). On the other hand, every particular ion "jumps" higher than, roughly, half of other ions, where it finds itself in the partially screened field. Exact solution of Poisson-Boltzmann equation indicates that these two factors cancel each other, yielding Eq. (3).

The next step of the screening story, well known to every physicist, is the theory of Debye and Hückel (1923) initially developed for electrolytes - the overall neutral mixture of mobile ions of both signs, and now widely used in plasma and solid state physics. Debye and Hückel realized that Poisson-Boltzmann equation (1) should be generalized by introducing the sum over ion species in the right-hand side, and then it can be linearized. Debye-Hückel screening leads to exponential decay of the potential around a point-like charge Q :

$$\phi(r) = \frac{Q}{\epsilon r} e^{-r/r_s}, \quad (4)$$

where the Debye-Hückel radius is given by

$$r_s = \left(\frac{k_B T}{8\pi N_1 e^2}\right)^{1/2}, \quad (5)$$

and N_1 is the concentration of monovalent salt.

The last step we mention here is relatively recent, it has to do with non-linear screening of cylindrical charges, such as DNA double helix (Onsager, 1967; Manning, 1969). Consider a cylinder charged to the linear density $-\eta$. Since the potential is logarithmic, its competition

with entropy is quite peculiar. Indeed, releasing counterions to some distance r requires energy $(2eZ\eta/\epsilon) \ln(r/a)$ (a being the cylinder radius), while the corresponding entropy gain is $k_B T \ln(\pi r^2/\pi a^2)$. Therefore, counterions are released only as long as $\eta < \eta_Z$, where

$$\eta_Z = k_B T \epsilon / eZ. \quad (6)$$

When a cylinder is charged in excess of $-\eta_Z$, some of the ions remain *Onsager-Manning condensed* on the cylinder, so that its effective net charge is equal to $-\eta_Z$. To emphasize the importance of this subject, let us mention that DNA double helix has bare charge density about $-4.2\eta_1$, where $\eta_1 = \eta_Z|_{Z=1}$. Onsager-Manning condensation was more accurately justified by Zimm and Le Bret (1983) by addressing non-linear Poisson-Boltzmann equation in cylindrical geometry.

It is worth mentioning that Gouy-Chapman, Debye-Hückel, and Onsager-Manning theories are all of mean field type, based on Poisson-Boltzmann equation. This approach applies well when screening charges are small. In the case of strongly charged macroions and Z -ions, correlations are important, mean field theory fails, and it is necessary to step beyond this approximation. This is precisely the subject matter of the present article. Charge inversion in this context should be viewed as the most obvious manifestation of the mean field failure.

III. STRONGLY CORRELATED LIQUID OF MULTIVALENT IONS

To begin with, let us explain why Gouy-Chapman solution (2) fails at large Z . Apart from λ (3), there is a second length scale in the problem due to the discreteness of charge, it is associated with the distance between ions in the lateral direction, along the plane. As long as the system as a whole is neutral, the two-dimensional concentration of Z -ions is $n = \sigma/Z\epsilon$, and the surface area per one ion can be characterized by the radius R such that $\pi R^2 = 1/n$ (see Fig. 5): $R = (\pi n)^{-1/2} = (Z\epsilon/\pi\sigma)^{1/2}$. It is not difficult to see that

$$\frac{R}{\lambda} = 2\Gamma, \quad \Gamma = \frac{Z^2 e^2 / \epsilon R}{k_B T}. \quad (7)$$

Here Γ is the Coulomb coupling constant, or the inverse dimensionless temperature measured in the units of typical interaction energy between Z -ions. The system of monovalent ions, $Z = 1$, is weakly coupled, $\Gamma \sim 1$, this is why classical mean field theory applies. By contrast, the system with large Z is strongly coupled, and we see that R becomes larger than λ . For example, at $Z = 3$ and $\sigma = 1.0 e/\text{nm}^2$ we get $\Gamma = 6.4$, $\lambda \simeq 0.1$ nm and $R \simeq 1.0$ nm. Clearly, mean field treatment along the lines of Poisson-Boltzmann theory fails in this situation, since Z -ions do not affect each other when they are at the

distances smaller than R from the plane. It is worth emphasizing once again that it is not the *linearized* Debye-Hückel theory that fails in the strong coupling regime, but so does also the non-linear Poisson-Boltzmann theory. It is the mean field approximation that is inapplicable because of correlations between discrete charges.

The alternative theory appropriate for the regime $\Gamma \gg 1$ was suggested by Perel and Shklovskii (1999). The main idea of this theory is that at $\Gamma \gg 1$ the screening atmosphere is narrowly confined at the surface (see Fig. 1), and it should be approximated as a two-dimensional SCL.

Two-dimensional liquid of classical charged particles on the neutralizing background, the so called one component plasma, is well understood (Totsuji, 1978). At zero temperature, it acquires the minimal energy state of a Wigner crystal, shown in the Fig. 5, in which the correlation energy per ion and the chemical potential read

$$\varepsilon(n) \simeq -1.11 Z^2 e^2 / R \epsilon = -1.96 n^{1/2} Z^2 e^2 / \epsilon, \quad (8)$$

$$\mu_{WC} = \frac{\partial[n\varepsilon(n)]}{\partial n} = \frac{3}{2}\varepsilon(n) = -1.65 Z^2 e^2 / \epsilon R. \quad (9)$$

We interpret R here as the radius of Wigner-Seitz cell approximated as a disc.

At non-zero temperature, the chemical potential of one component plasma can be written as $\mu = \mu_{id} + \mu_{WC} + \delta\mu$. Here μ_{id} corresponds to ideal gas, or, equivalently, to randomly positioned Z -ions. Accordingly, $\mu_{WC} + \delta\mu$ part is entirely due to correlations. Furthermore, it turns out that $\delta\mu$, which is the thermal (entropy-related) contribution, is negligible at $\Gamma \gg 1$. Although Wigner *crystal*, in terms of long range order, melts at $\Gamma \approx 130$, the value of $\delta\mu$ is controlled by short range order and remains negligible as long as $\Gamma \gg 1$. It is in this sense that SCL of Z -ions is similar to Wigner crystal.

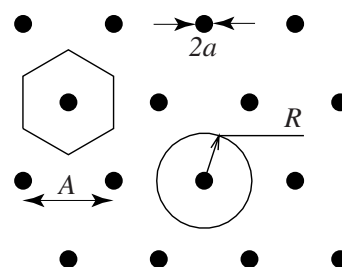


FIG. 5. The Wigner crystal of positive Z -ions on the negative uniform background of surface charge. A hexagonal Wigner-Seitz cell and its simplified version as a disk with radius R are shown.

Thus, the correlation part of chemical potential is approximated as μ_{WC} (9) which is negative and large: $-\mu_{WC}/k_B T = 1.65\Gamma \gg 1$. Physics of a large and negative μ_{WC} can be understood as follows. Pretend for a moment that the insulating macroion is replaced by a neutral metallic particle. In this case, each Z -ion creates

an image charge of opposite sign inside the metal. Energy of attraction to the image is $U(x) = -(Ze)^2/4\epsilon x$, where x is the distance to the surface. This energy is minimal when Z -ion is placed next to the surface, at the distance equal to its radius a ; therefore, Z -ions sticks to the surface. With this idea in mind, consider bringing a new Z -ion to the insulating macroion surface already covered by an adsorbed layer of Z -ions (Fig. 6). This layer behaves like a metal surface in the sense that the new Z -ion repels adsorbed ones, creating a correlation hole. In other words, it creates a negative image. Because of the discreteness of charges, adsorbed layer is a good metal at the length scales above R only. Accordingly, attraction to the image gets saturated at $x \sim R$ and this is why chemical potential of ion in Wigner crystal scales as $\mu_{WC} \sim -(Ze)^2/\epsilon R$. Eq. (9) specifies the numerical coefficient in this expression.

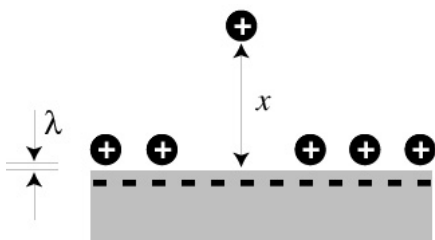


FIG. 6. The origin of attraction of a new positive Z -ion to the already neutralized surface. Z -ions are shown by solid circles. The new Z -ion creates its negative correlation hole.

Using the concept of images, we can now understand the distribution of Z -ions, $N(x)$, near the surface. To do this, let us extract one Z -ion from SCL and move it along the x axis. As long as $x \ll R$, its correlation hole does not change, and, therefore, Z -ion is attracted to the surface by the uniform electric field $E = 2\pi\sigma/\epsilon$; other Z -ions do not affect this attraction in any way. Therefore, $N(x) = N_s \exp(-x/\lambda)$ at $x \ll R$. Here $N_s \simeq n/\lambda$ is the three-dimensional concentration of Z -ions at the plane (Eq. (1)). At $x \gg R$, the correlation hole acts as a point-like image charge, the corresponding interaction energy being $-Z^2e^2/4\epsilon x$. At $x = Z^2e^2/4\epsilon k_B T = R_0\Gamma/4 = \lambda\Gamma^2/2$, interaction with image drops to about $k_B T$, becomes negligible, and Z -ions concentration reaches the value

$$N_0 = N_s \exp\left(-\frac{|\mu_{WC}|}{k_B T}\right) = N_s \exp\left(-\frac{1.65Z^2e^2}{\epsilon R k_B T}\right). \quad (10)$$

Note that the correction term $-Z^2e^2/4\epsilon x$ in Z -ion energy, operational in the interval $R \ll x \ll \lambda\Gamma^2/2$, is similar to the "image" correction to the work function of a metal (Lang, 1973).

The dramatic difference between the exponential decay of $N(x)$ and the Gouy-Chapman $1/(\lambda+x)^2$ -law (2) is due to the correlation effects. Moreira and Netz (2000a) re-derived these results in a more formal way and confirmed them by Monte-Carlo simulations.

At larger x , correlations and interaction with image charge are unimportant, and Poisson-Boltzmann equation applies. In this region $N(x)$ varies so smoothly that $N(x) = N_0$ provides an effective boundary condition for the Poisson-Boltzmann equation (Shklovskii, 1999b). At this stage we must remember that in the real physical situation there is always some concentration of salt in the surrounding solution. Accordingly, N_0 may be either larger or smaller than the bulk concentration of the Z -ions, N ; in the latter case, the surface is overcharged, as we show in the Sec. IV below.

IV. CORRELATION-INDUCED CHARGE INVERSION

We are now in a position to formulate the problem of correlated screening, central for this review. Consider a single macroion in a macroscopic solution which contains $Z : 1$ salt (such as, e.g., LaCl_3) with concentration N (each molecule of $Z : 1$ salt dissociates into one Z -ion and Z monovalent ions of the opposite sign; there are also neutralizing monovalent counterions dissociated from the macroion). Postponing the issue of monovalent salt till the next Sec. V, we ask: how do Z -ions screen the macroion charge? This question is non-trivial in the light of our findings in the previous Sec. III. Indeed, as we have established, Z -ions of the two-dimensional SCL are strongly attached to the macroion surface, such that $|\mu_{WC}| \gg k_B T$. Accordingly, their complex with the macroion represents an integral body - they move together, both in Brownian motion and when drifting in the weak field electrophoresis. Therefore, the question of screening boils down to this: how many Z -ions are attached to the macroion? In other words, what is the total charge of the complex, Q^* (or surface charge density σ^*)? In particular, if Q^* (or σ^*) has opposite sign compared to macroion bare charge $-Q$ (or $-\sigma$), we deal with charge inversion. Clearly, to determine Q^* (or σ^*) we must address the density n of SCL: $\sigma^* = -\sigma + Zen$. Physically, this density is governed by the equilibrium with the surrounding solution.

Let us see how we can use the chemical potential of a neutral one component plasma (9) when the surface is not neutral, $\sigma^* \neq 0$. For simplicity, let us concentrate on the spherical macroion with uniformly charged surface, and also assume a negligible concentration of monovalent salt, when $r_s \rightarrow \infty$ according to Eq. (5). Pretend to add two uniformly charged surfaces, with densities $-\sigma^*$ and σ^* , to the macroion surface. The charge $-\sigma^*$ along with SCL is a neutral one component plasma, for which Eq.

(9) directly applies. The other charge, σ^* creates only a constant potential, $\psi(0) = Q^*/\epsilon r$, on the macroion surface (since $r_s \rightarrow \infty$). It is important to emphasize that macroscopic net charge σ^* does not interact with one component plasma, because potential $\psi(0)$ is constant along the surface, and one component plasma is neutral.

The equilibrium condition between SCL and the bulk solution reads $\mu_{id} + \mu_{WC} + Ze\psi(0) = \mu_b$, where μ_b is the bulk chemical potential. The terms can be conveniently rearranged to yield $Ze\psi(0) = -\mu_{WC} + (\mu_b - \mu_{id}) = -\mu_{WC} + k_B T \ln(N_s/N) = k_B T \ln(N/N_0)$ or

$$Q^* = \frac{\epsilon r}{Ze} k_B T \ln(N/N_0). \quad (11)$$

Clearly, the net charge density Q^* is indeed positive when $N > N_0$, i.e. it has the sign opposite to the bare charge density Q . The concentration N_0 , as defined by Eq. (10), is very small because $|\mu_{WC}|/k_B T \gg 1$. For example, $N_0 = 0.3$ mM and 0.8 μ M for $Z = 3$ and 4 respectively ($1 \text{ M} \approx 6 \times 10^{20} \text{ cm}^{-3}$). Therefore, it is easy in practice to achieve charge inversion by increasing N . How far does it go? At large enough N , translational entropy terms $|\mu_b - \mu_{id}|$ become negligible compared to $|\mu_{WC}|$, yielding

$$\psi(0) = |\mu_{WC}|/Ze. \quad (12)$$

Expressing R and $|\mu_{WC}|$ through Q and Z with the help of Eq. (9), Shklovskii (1999b) arrived at the prediction for the inverted charge for the spherical macroion screened by a large concentration of $Z : 1$ salt:

$$Q^* = 0.83\sqrt{QZe}. \quad (13)$$

Eqs. (12) or (13) determine the maximal charge inversion achievable without a monovalent salt (see Sec V). This charge is much larger than Ze , but still is smaller than Q because of limitations imposed by the large charging energy of the macroscopic net charge. For example, for $Q = 100e$, $Z = 4$, we get $Q^* = 17e$. Eq. (13) was recently confirmed by numerical simulations (Messina et al, 2000; Tanaka and Grosberg, 2001a).

Applied in cylindrical geometry, similar arguments lead to the revision of the conventional Onsager-Manning condensation theory (Sec. II) when dealing with multivalent Z -ions. Consider a cylinder with a negative linear charge density $-\eta$ and assume that $\eta > \eta_z$. Mean field Onsager-Manning theory (6) predicts $\eta^* = -\eta_z$. By contrast, Perel and Shklovskii (1999) showed that correlation induced negative chemical potential μ_{WC} results in

$$\eta^* = -\eta_z \frac{\ln(N_0/N)}{\ln\left(4(\epsilon k_B T)^3 / \pi(Ze)^6 N\right)} \quad (14)$$

(compare with Eq. (11) for the sphere). This result reproduces the Onsager-Manning one (6) only at extremely small values of N , which are unrealistic at $Z \geq 3$. On the other hand, at $N = N_0$ the net charge flips sign, resulting in charge inversion at $N > N_0$. At large enough N , the inverted charge density η^* can reach $k_B T \epsilon / e = \eta_1$.

V. ENHANCEMENT OF CHARGE INVERSION BY MONOVALENT SALT

Most of water solutions, particularly biological ones, contain significant amount of monovalent salt, such as NaCl. Correlations between these monovalent ions are negligible, and, therefore, their role is Debye-Hückel screening with the decay length r_s (5). This screening makes charge inversion substantially stronger. Indeed, screening by a monovalent salt diminishes the charging energy of the macroion much stronger than the correlation energy of Z -ions. Furthermore, in a sufficient concentration of salt, the macroion is screened at the distance smaller than its size. Then, the macroion can be thought of as an over-screened surface, with inverted charge Q^* proportional to the surface area. In this sense, overall shape of the macroion is irrelevant, at least to a first approximation. Therefore, we consider here a simpler case: screening of a planar macroion surface with a negative surface charge density $-\sigma$ by a solution with a concentration N of $Z : 1$ salt and a large concentration N_1 of a monovalent salt.

Nguyen et al (2000a) calculated analytically the dependence of the charge inversion ratio, σ^*/σ , on r_s , in two limiting cases $r_s \gg R_0$ and $r_s \ll R_0$, where $R_0 = (\pi\sigma/Ze)^{-1/2}$ is the radius of a Wigner-Seitz cell at the neutral point $n = \sigma/Ze$. At $r_s \gg R_0$ calculation starts from Eq. (12). The electrostatic potential of a plane with the charge density σ^* screened at the distance r_s reads $\psi(0) = 4\pi\sigma^*r_s$. At $r_s \gg R_0$ screening by monovalent ions does not change Eq. (9) substantially so that we still can use it in Eq. (12) which now describes charging of a plane capacitor by voltage $|\mu_{WC}|/Ze$. This gives

$$\sigma^*/\sigma = 0.41(R_0/r_s) \ll 1 \quad (r_s \gg R_0). \quad (15)$$

Thus, at $r_s \gg R_0$ inverted charge density grows with decreasing r_s .

Now we switch to the case of strong screening by monovalent salt, $r_s \ll R_0$. It seems that in this case σ^* should decrease with decreasing r_s , because screening reduces the energy of SCL of Z -ions and leads to its evaporation. Indeed, eventually this happens. However, there is a range where $r_s \ll R_0$, but the energy of SCL is still greater than $k_B T$ per Z -ion. In this range, as r_s decreases, the repulsion between Z -ions becomes weaker, so that it is easier to pack more Z -ions on the plane. Therefore, σ^* continues to grow with decreasing r_s . In this regime, all interactions are Debye-Hückel screened, so that interaction of non-nearest neighbors can be neglected. Therefore, free energy consists of nearest neighbor repulsion energies of Z -ions and the attraction energy of Z -ions to the charged surface:

$$F = (3nZ^2e^2/\epsilon A) \exp(-A/r_s) - 4\pi\sigma r_s Zen/\epsilon, \quad (16)$$

where $A = (2/\sqrt{3})^{1/2}n^{-1/2}$ is the lattice constant of the hexagonal Wigner crystal (Fig. 5). Minimizing F with respect to n one arrives at

$$\frac{\sigma^*}{\sigma} = \frac{\pi}{2\sqrt{3}} \left(\frac{R_0}{r_s \ln(R_0/r_s)} \right)^2 \quad (r_s \ll R_0). \quad (17)$$

Thus σ^*/σ grows with decreasing r_s and can become larger than 100%. At $r_s \sim R_0$, Eq. (15) and Eq. (17) match each other.

Terao and Nakayama (2001) reported the results of Monte Carlo simulation for the system consisting of a macroion with charge $Q = 20e$ surrounded by 20 monovalent counterions and 1500 ions of either 2 : 1 or 2 : 2 electrolyte. Tanaka and Grosberg (2001a) performed molecular dynamics simulations with a spherical macroion of the charge $Q = 30e$, spherical Z -ions ($Z = 2 \div 7$), and up to 500 monovalent ions of both signs. Simulations confirmed the strong adsorption of the overcharging amount of Z -ions on the surface of macroion. On a more quantitative level, Tanaka and Grosberg (2001a) examined the dependence of the inverted charge on the ionic strength, I , and found the crossover between $Q^* \propto \sqrt{I} \propto 1/r_s$ and $Q^* \propto I \propto 1/r_s^2$, consistent with Eqs. (15) and (17). Tanaka and Grosberg (2001a) attempted also to maximize charge inversion ratio Q^*/Q . In agreement with the theoretical views presented above, the growth of charge inversion is capped when correlations between Z -ions are suppressed. We have mentioned eventual reduction of correlations for large monovalent salt concentration, or small r_s , when SCL evaporates. If one tries to increase Z instead of lowering r_s , then, at large Z , correlations become suppressed because monovalent ions start to condense on Z -ions, effectively reducing Z . Nevertheless, Q^*/Q up to about 150% is easily observed. In a more recent simulation, Tanaka and Grosberg (2001b) have also confirmed that adsorbed Z -ions drift together with the macroion in a weak electric field.

VI. SCREENING OF A CHARGED PLANE BY POLYELECTROLYTES

A practically important class of Z -ions are charged polymers - polyelectrolytes. Let us start with a rigid polyelectrolyte and discuss charge inversion caused by adsorption of long rod-like Z -ions. For example, moderately long (up to about 50 nm, or about 150 base pairs) DNA double helix is very well approximated as a rod. Actin is another example of even more rigid polyelectrolyte. Apart from the uninteresting regime of extremely small macroion surface charge density (in which case elongated shape of molecules is irrelevant, rendering our previous results applicable), charged rods adsorbed at the surface tend to be parallel to each other due to the strong lateral repulsion. In other words, there is a short range order of

an one-dimensional Wigner crystal with lattice constant A in the direction perpendicular to rods (Fig. 7).

To make signs consistent with the case of DNA, we assume that the polyelectrolyte charge is negative and equal to $-\eta$ per unit length, while the macroion surface is a plane with positive charge density σ . We assume also that there is certain concentration of monovalent salt, N_1 , in the solution, corresponding to the Debye screening radius (5). To begin with, let us assume that rods charge density $-\eta$ is below the Onsager-Manning threshold, Eq. (6), and let us apply the Debye-Hückel approximation to describe screening of the charged surface by monovalent salt. We can then directly minimize the free energy of one-dimensional crystal of negative rods on the positive surface written similarly to Eq. (16). Then the competition between attraction of rods to the surface and the repulsion of the neighboring rods results in the negative net surface charge density $-\sigma^*$ similar to Eq. (17) (Netz and Joanny, 1999a; Nguyen et al, 2000a):

$$\frac{\sigma^*}{\sigma} = \frac{\eta/\sigma r_s}{\ln(\eta/\sigma r_s)}, \quad r_s \ll A_0. \quad (18)$$

Here the applicability condition involves $A_0 = \eta/\sigma$ - the distance between rods when they neutralize the plane; only at $r_s \ll A_0$, the overcharged plane is linearly screened by monovalent salt.

Speaking about DNA, we have already discussed in Sec. II that DNA charge, $-\eta$, is such that about three quarters of it is compensated by positive Onsager-Manning-condensed monovalent ions. In other words, the net charge of DNA in the bulk solution is $\eta^* = -\eta_1$ (6). It turns out that at $r_s \ll A_0$ the result (18) applies to DNA with the only correction of replacing $-\eta$ with $\eta^* = -\eta_1 \equiv -k_B T \epsilon / e$ (Nguyen et al, 2000a).

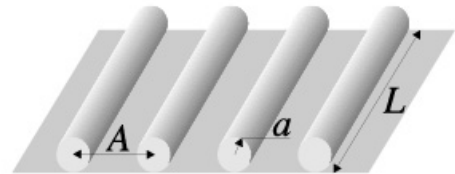


FIG. 7. Rod-like negative Z -ions, adsorbed on a positive uniformly charged plane.

Thus the inversion ratio grows with decreasing r_s as in the case of spherical Z -ions. At small enough r_s and σ , the inversion ratio can reach 200% before DNA molecules are released from the surface. It is larger than for spherical ions, because in this case, due to the large length of DNA helix, the correlation energy remains large and Wigner crystal-like short range order is preserved at smaller values of σr_s . Nguyen et al (2000a) called this phenomenon "giant charge inversion."

Let us switch now to the opposite extreme of weak screening by a monovalent salt, $r_s \gg A_0$. In this case, screening of the overcharged plane by monovalent salt becomes strongly nonlinear, with the Gouy-Chapman screening length $\lambda^* = \epsilon k_B T / (2\pi e \sigma^*)$ much smaller than r_s . Furthermore, some of the positive monovalent ions Onsager-Manning condensed on DNA are released from it upon adsorption, as plane repels them (Park et al, 1999; Gelbart et al, 2000). As a result the absolute value of the net linear charge density of each adsorbed DNA, η^* , becomes larger than η_1 . To determine σ^* and η^* , Nguyen et al (2000a) considered two equilibrium conditions, dealing with chemical potentials of rods and small ions, respectively. As a result, they arrived at the following solution valid at $r_s \gg A_0$:

$$\frac{\sigma^*}{\sigma} = \frac{\eta_1}{2\pi a \sigma} \exp\left(-\sqrt{\ln \frac{r_s}{a} \ln \frac{A_0}{2\pi a}}\right), \quad (19)$$

$$\eta^* = \eta_1 \sqrt{\frac{\ln(r_s/a)}{\ln(A_0/2\pi a)}}, \quad r_s \gg A_0. \quad (20)$$

At $r_s \simeq A_0/2\pi$ we get $\eta^* \simeq \eta_1$, $\lambda^* \simeq r_s$ and $\sigma^*/\sigma \simeq \eta_1/(2\pi r_s \sigma)$ so that Eq. (19) crosses over smoothly to the strong screening result of Eq. (18).

So far in this Section we assumed a rod-like polyelectrolyte. Let us now discuss how chain flexibility affects charge inversion. We argue that the results for rod-like Z -ions are remarkably robust. To begin with, consider polyelectrolyte having several charged groups per each persistence length. We argue that our results remain valid as long as adsorption energy *per one persistence length* is large compared to $k_B T$. Indeed, under this condition even flexible polyelectrolyte chains lay flat on the surface, in which case they are ordered in Wigner crystal-like SCL and, therefore, behave similarly to rods.

Dobrynin et al (2001) addressed the opposite extreme, namely, weakly charged polyelectrolytes, with so small fraction of charged monomers, f , that a link between two neighboring charges is already a flexible polymer; in other words, the distance between charges is larger than the persistence length. As the reader may remember (de Gennes et al, 1976), weakly charged polyelectrolyte chain in a bulk solution consists of electrostatic blobs, such that inside each blob chain statistics is only marginally perturbed by Coulomb interactions, while chain of blobs is fully stretched, rod-like. Dobrynin et al (2001) have found that this blob structure remains valid for the adsorbed chains, which form SCL of effective rods of blobs. Speaking of charge inversion, this means that the Eq. (18) remains valid for the weakly charged chains, provided η is replaced with linear charge density of the string of blobs $\eta^* = (f\epsilon e k_B T / l^2)^{1/3}$, where l is the chain persistence length, and r_s is larger than a blob size.

With increasing σ , adsorbed rods, either real or blob ones, start to touch each other leading to multilayer adsorption. It is only in this regime that the real and blob rods behave differently, as we discuss in the Sec. VIII.

VII. POLYELECTROLYTES WRAPPING AROUND CHARGED PARTICLES

As we have mentioned in the Introduction, one of the practically important situations is that of a long charged polymer forming complexes with oppositely charged particles. Motivated by the problem of nucleosome charge inversion, Mateescu et al (1999), Park et al (1999), Sens and Gurovich (1999), Netz and Joanny (1999b) considered the complex of a positive sphere with charge q and a negative polyelectrolyte, such as DNA double helix, which has to make some $m > 1$ turns around the sphere to neutralize it (Fig. 8). These authors predicted a substantial charge inversion: more of polyelectrolyte is wound than necessary to neutralize a sphere. Furthermore, Mateescu et al (1999) found that tightly coiled polyelectrolyte conformation becomes unstable when chain length exceeds certain threshold, and then an almost straight tail abruptly stretches out (Fig. 8).

Nguyen and Shklovskii (2001a) emphasized the role of correlations in this case of charge inversion. Indeed, neighboring turns repel each other and form an almost equidistant solenoid, which locally resembles SCL. The tail of polyelectrolyte repels the already adsorbed part of polyelectrolyte and creates a correlation hole, which attracts the tail back to the surface (compare Fig. 6). As a result, the net charge of the sphere with wrapped polyelectrolyte, q^* , is negative. It is shown that at $r_s \rightarrow \infty$ the charge inversion ratio scales as $|q^*|/q \sim 1/m$. On the other hand, at small enough r_s it can exceed 100%.

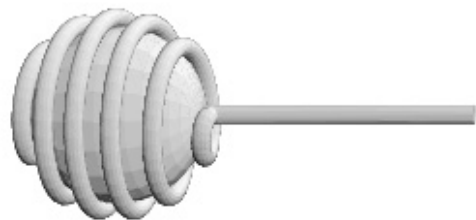


FIG. 8. A polyelectrolyte molecule winding around a spherical macroion. Due to the Coulomb repulsion, neighboring turns, which play the role of Z -ions, are strongly correlated.

Even more interesting is the system in which charged polymer is so long that it forms complexes with many oppositely charged particles (see Fig. 4). Examples include micelles (Wang et al, 1999), globular proteins (Kabanov et al, 1976; Xia and Dubin, 1994), colloids (Braun et al, 1998; Keren et al, 2001), or dendrimers (Evans et al, 2001), and, last but not least, histone octamers form-

ing 10 nm chromatine fiber with DNA (Fig. 3). To be specific, we remain with the signs consistent with the DNA case and consider a long negative polymer chain in the solution of positive spheres. If the concentration of spheres is large, it is favorable to adsorb many spheres on the polyelectrolyte chain. As a result, each sphere is under-screened by polyelectrolyte and has positive net charge. Then, adsorbed spheres repel each other and the complex forms a periodic necklace (see Fig. 4). This necklace is, in fact, a one-dimensional Wigner crystal, or SCL, of spheres, which serve as Z -ions. Indeed, since the segment of the polyelectrolyte wound around one sphere interacts almost exclusively with this sphere, it plays the role of the Wigner-Seitz cell. Because of correlations, spheres bind to polyelectrolyte in such a large number that the net charge of the polyelectrolyte molecule becomes positive (Nguyen and Shklovskii, 2001b). In this case, charge inversion ratio scales as $Q^*/Q \sim m^{1/4}$ in the absence of monovalent salt, where $-Q$ and Q^* are the bare and net charges of the polyelectrolyte molecule, respectively. This means, charge inversion may be larger than 100%. As we discussed in Sec. V, charge inversion can be further enhanced by a monovalent salt, in which case $Q^*/Q \sim m$. We shall return to the complexes of charged chain with spheres in the Sec. IX.

VIII. MULTILAYER ADSORPTION

So far we did not consider the possibility that Z -ions fully cover the macroion surface. Meanwhile, this may sometimes happen, particularly when macroion is very strongly charged, or Z -ions are large. Suppose, for instance, that each Z -ion has a hard core of some radius a . In this case, excluded volume effect of hard cores of Z -ions adds a positive contribution to the chemical potential of SCL (9), which is proportional to $k_B T$ and diverges at the full coverage along with the surface pressure. Close to the full layer this term compensates and then over-compensates the negative Coulomb term μ_{WC} , so that charge inversion disappears. Indeed, full layer is incompressible (see Fig. 9b), and, unlike partially filled layer (see Fig. 6 or Fig. 9a), it does not allow for the creation of correlation hole and image.

At even larger macroion charge, the second layer starts to form, launching a new wave of charge inversion. In the beginning, charge inversion is small because all the attraction of a new Z -ion approaching the surface is provided by a weak interaction with an inflated image in the emerging second layer, where once again $A \gg a$ (Fig. 9c). Continuing, Nguyen and Shklovskii (2001c) arrived at the prediction of oscillating inverted charge Q^* as a function of Q (see Fig. 9), where charge inversion vanishes every time the top layer of Z -ions is full.

Another way to look at this phenomenon is to examine a metallic electrode screened by Z -ions, when the poten-

tial of the electrode is controlled instead of its charge. In this case, oscillations of charge inversion and compressibility lead to oscillations of capacitance of this electrode with the number of adsorbed layers of Z -ions. This is similar to oscillations of compressibility and magneto-capacitance in the quantum Hall effect, which are related to consecutive filling of Landau levels (Efros, 1988; Kravchenko et al, 1990; Eisenstein, 1992). In this sense, we deal with a classical analog of the quantum Hall effect.

To conclude this section, let us return to the adsorption of weakly charged polyelectrolytes briefly discussed in the Sec. VII. Dobrynin et al (2001) have shown that parallel chains of adsorbed blobs start touching each other above the same threshold surface charge density $\sigma_e = ef/l^2$, which corresponds to the onset of squashing blobs on the surface. As a result, these authors arrived at the conclusion that at $\sigma > \sigma_e$ adsorbed weakly charged chains form a polymer liquid such that correlations and image formation are only due to the uppermost layer, with the thickness about that of an unperturbed blob. There are no oscillations of inverted charge; instead, charge inversion saturates at about one layer of blobs and remains unchanged afterwards.

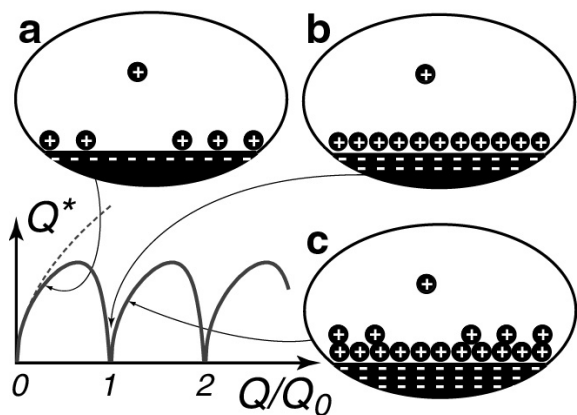


FIG. 9. Inverted charge Q^* as a function of the absolute value Q of the bare charge; Q_0 is the charge of one full layer of Z -ions. Dashed line corresponds to Z -ions with vanishing radius, Eq. (13). (a) The first layer is not full, like in Fig. 6. Approaching new ion creates correlation hole and attracts to it. (b) The layer is full, there is no place for correlation hole. (c) More than one layer is full. Correlation hole exists in the top layer only.

IX. CORRELATION INDUCED ATTRACTION OF LIKE CHARGES

The idea of a single screened macroion is a useful one in theoretical context, but in practice it is rarely true that there is only one macroion. Typically, there is certain concentration of them, so that interactions between them can be important. Let us start with the simplest

question: consider two macroions, and suppose the concentration of Z -ions in solution is equal to N_0 (see Eq. (10)), such that each macroion forms a neutral complex with Z -ions. How do these two neutral complexes interact? It turns out that they attract each other at short distances and, therefore, tend to coalesce. In other words, like charged macroions attract each other because of the presence of Z -ions. In general, this attraction of like charges is as interesting manifestation of correlations as charge inversion, even though our present review is biased towards charge inversion. Nevertheless, we must discuss attraction at least briefly, to prepare grounds for the subsequent discussion of experiments (Sec. X).

Medium induced attraction of like charges is nothing new in physics, Cooper pairs of electrons being the most prominent example. In the context of molecular physics, the most popular explanation of attraction is in terms of *salt bridges*: divalent ion, such as Mg^{2+} , can connect two groups with charges -1 each. This idea is indeed quite good if we have, say, two macroion surfaces with regularly placed charges -1 , and there are ions $+2$ between them. However appealing, bridge concept becomes increasingly fuzzy when Z -ions have charges 3 or higher and when charges in the macroion are not positioned regularly.

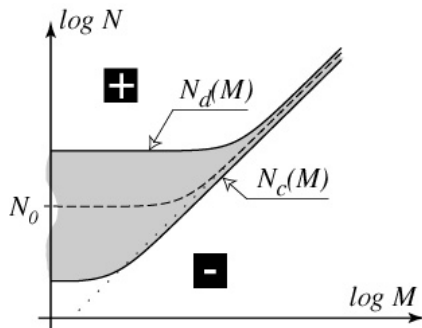


FIG. 10. Generic phase diagram of reentrant condensation and charge inversion in terms of macroion concentration M and Z -ions concentration N (Nguyen and Shklovskii, 2001d). Isoelectric composition is shown by dotted line. The dashed "neutrality line" corresponds to neutral complexes in the dilute phase. Segregation region is shaded. Minus and plus indicate the signs of complexes of DNA with Z -ions.

Motivated by experimental observations of DNA condensation (see Sec. X), there was a significant effort of the theorists trying to explain attractive forces beyond the bridge model. For simplicity, and following the majority of works, let us consider two planar macroion surfaces with some Z -ions between them. Of course, Poisson-Boltzmann theory predicts pure repulsion for such system. However, attraction was observed in several computer experiments, including Guldbbrand et al (1984), Kjellander and Marcelja (1985), Gronbech-Jensen (1997), Linse and Lobaskin (1998), and Moreira and Netz (2000b). Theoretically, several groups at-

tempted to go beyond the mean field approximation. An important observation is that due to dynamic fluctuations of counterions in a neutralizing solution, there is even an attractive component (similar to Van der Waals interactions), but the force remains mainly repulsive (Oosawa, 1968; Lau and Pincus, 1998; Ha and Liu, 1998; Podgornik and Parsegian, 1998; Golestanian et al, 1999; Golestanian and Kardar, 1999).

It turns out that the idea of spatial correlations between Z -ions, which is the central idea of this review, sheds light on the nature of strong short range attractions between like charges. For extremely large Γ (see Eq. (7) for the definition of Γ), we deal with two Wigner crystals on the two opposing plates, they gain energy when approach each other by properly positioning themselves in the lateral direction. This was shown by Rouzina and Bloomfield (1996) (see also Gronbech-Jensen, 1997; Levin et al, 1999; Moreira and Netz, 2000b). Furthermore, Shklovskii (1999a) pointed out that long range order of a Wigner crystal is not important for this attraction force. Like in the case of charge inversion, what is important is correlation and short range order. As we know, Z -ions form SCL on the macroion surface as soon as Γ becomes large. When two surfaces come close, their SCL merge, lowering energy per Z -ion from $\varepsilon(n)$ to $\varepsilon(2n) < \varepsilon(n)$ (see Eq. (8)). Physically, every Z -ion in the merged SCL is sandwiched between *two* discs, one from each macroion surface, and these two together form Wigner-Seitz cell. The charge of the cell is still $-Ze$, but its radius is reduced by the factor $1/\sqrt{2}$, leading to the energy gain. In some sense, this theory returns us to the idea of bridges, albeit on a completely new level, each Z -ion bridging between two sides of its Wigner-Seitz cell, which can include many surface charges.

These arguments hold, at least qualitatively, not only for plates, but also for macroions of other shapes, including DNA double helices. To be specific, consider two DNA double helices. When concentration of Z -ions is equal to N_0 , each DNA is neutralized by Z -ions, and the two neutral complexes attract each other at short distances. What happens if concentration of Z -ions is higher or lower than N_0 ? In this case, correlation-induced attraction, which is short ranged, competes with Coulomb repulsion, which is much longer ranged. Note, that the Coulomb repulsion force is present both at $N < N_0$, when DNA's are partially screened by Z -ions and negative, and at $N > N_0$, when they are overcharged and positive.

What are the implications of this competition between attraction and repulsion? They are summarized in the Fig. 10 which shows phase diagram of the solution with number concentrations of macroions, M , and Z -ions, N (along with neutralizing amount of monovalent ions and salt.) The major feature of the phase diagram is the segregation region, which is the shaded area in the Fig. 10. As the figure indicates, the generic scenario is that

of *reentrant condensation*. DNA stays in solution and remain negative at $N < N_c(M)$, forming undercharged complexes with Z -ions. At some concentration of Z -ions, $N = N_c(M)$, repulsion looses to the correlation attraction and condensed phase of DNA is formed, coexisting with a dilute phase. Condensed phase for DNA represents a (nematic) bundle of helices, it exists in the interval $N_c(M) < N < N_d(M)$. Finally, at $N = N_d(M)$, repulsion overcomes correlation attraction, DNA dissolves and forms positive (overcharged) complexes with Z -ions.

Inside the coexistence region, there is a neutrality line, on which the equilibrium dilute phase consists of *neutral* complexes. At very small DNA concentration, the neutrality condition corresponds to concentration N_0 of Z -ions (Eq. 10). To see what happens at larger DNA concentration, consider increasing M starting from the overcharged complexes, well above segregation on the phase diagram Fig. 10. When M grows, the solution runs out of Z -ions when it approaches the "isoelectric line" $-\eta LM + ZeN = 0$, $-\eta < 0$ and L being the DNA linear charge density and length, respectively. Near this line, charge of complexes flips sign. Thus, the neutrality line crosses over from $N = N_0$ to the isoelectric line. Border lines $N_c(M)$ and $N_d(M)$ follow a similar pattern. Of course, at a extremely small M these two lines join together at a critical point, and at smaller M only intramolecular condensation of DNA, or coil-globule transition, is possible if DNA is long enough.

We considered phase diagram Fig. 10 for a solution of DNA chains with small Z -ions, such as spermine. As a matter of fact, the diagram is qualitatively quite general (Nguyen and Shklovskii, 2001d). For instance, it applies to the solution of DNA with large positively charged particles. In Sec. VII, we considered small DNA concentration, M , and large concentration of spheres, N , which corresponds to the region above the coexistence region on the phase diagram Fig. 10. We found that complexes have a form of necklaces, as shown in Fig. 4, and they are overcharged by spheres. Large spheres are so strongly bound to DNA that concentration N_0 for them is extremely small and any real experiment deals with the narrow upper-right part of the diagram. Suppose now that there are relatively few spheres in the solution, so we are below the neutrality line. In this situation, chains make an overcharging number of turns around each sphere. This is energetically favorable due to the repulsive correlations between subsequent turns on a sphere surface. The inverted net charge of each sphere is about as large as for a single sphere discussed in Sec. VII. Furthermore, the inverted charge of spheres determines their distribution along the chain of polyelectrolyte. Negative spheres repel each other and, therefore, the complex once again has the periodic beads-on-a-string structure, Fig. 4, which resembles the 10 nm chromatin fiber. In the narrow vicinity of the neutrality line, even a small corre-

lation attraction between touching spheres is sufficient to provide aggregation of neutral DNA-spheres complexes or coil-globule collapse of a long DNA with spheres.

X. EXPERIMENTAL EVIDENCE OF CHARGE INVERSION

How does the theory of correlated screening compare with the experiment? For the purposes of this review, we restrict ourselves with the qualitative comparison only.

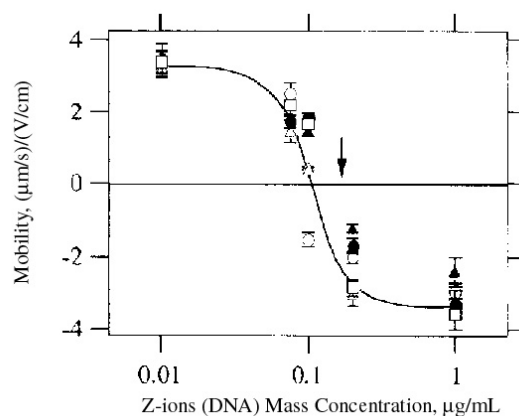


FIG. 11. Mobility of positive latex particles (macroions) in the presence of 0.005 M concentration NaCl as a function of polymer mass concentration. Polymers (single stranded DNA chains) play the role of Z -ions. Different symbols correspond to DNA of the following lengths (in monomers): \blacktriangle - 8, \circ - 10, \triangle - 40, \bullet - 80, \square - 1400. The line is drawn as a guide for an eye. The arrow shows to isoelectric point, the polymer mass concentration of $0.17 \mu\text{g ml}^{-1}$ at which DNA charge neutralizes that of latex particles.

Speaking about direct manifestations of charge inversion, the conceptually easiest way to see them is the reversal of the electrophoretic mobility of a macroion at certain concentration of $Z : 1$ salt. Wang et al (1999) observed such reversal for a mixture of polyelectrolytes (macroions) and micells (Z -ions). Gotting et al (1999) found the reversed mobility for the nanoparticles (macroions) and short single stranded DNA (elongated Z -ions). Walker and Grant (1996) demonstrated this phenomenon for 120 nm latex particles (macroions) with single stranded DNA (Z -ions) ranging from 8 to 1400 nucleotides; their data are presented in Fig. 11. Recently, Evan et al (2001) observed the reversed electrophoretic mobility for DNA with the dendrimers as Z -ions.

An interesting observation, apparent from the Fig. 11, is that the data for different DNA lengths collapse on a single master curve upon re-scaling in which mobility is plotted against mass concentration of DNA instead of number concentration, N . This observation can be rationalized by noting that mass concentration is basically

the same as the number of charged groups per unit volume which determines the isoelectric point insensitively to the overall length of elongated Z -ions - DNA.

For a more detailed and meaningful comparison, we should remember that charge reversal is expected to be accompanied by coagulation, as discussed above in the Sec. IX. Whether equilibrium or not quite equilibrium, these large complexes should scatter light strongly. There are many experiments reporting such observations.

Let us begin with DNA. It was known for some time already that at some critical concentration, N_c , DNA abruptly condenses into large bundles (Bloomfield, 1996). Recently it was discovered that at a much larger critical concentration, N_d , bundles dissolve back (Saminathan et al, 1999; Pelta et al, 1996a; Pelta et al, 1996b; Raspaud et al, 1998; Raspaud et al, 1999). Specifically, for the spermine ions ($Z = 4$), it was found experimentally that $N_c = 0.025$ mM and $N_d = 150$ mM. According to the theory of Nguyen et al (2000c), these experimental values of N_c and N_d imply that, for spermine, $N_0 = 3.2$ mM and the binding energy of two helices per one spermine ion is $u = 0.3k_B T$. The last value agrees with the one obtained by a different method (Rau and Parsegian, 1992).

Let us now discuss some other systems. Wang et al (1999) studied complexation in mixture of micelles and oppositely charged polyelectrolyte. In this experiment, the total charge of micelles was controlled by changing the concentration of the cationic lipid in the solution. In agreement with the above theory, measurements of dynamic light scattering and turbidity (coefficient of light scattering) show that complexes condense in bundles and solution coacervates in the vicinity of the point where mobility crosses over between two almost constant values, positive and negative.

For the complexes of latex particles with DNA of various lengths, examined by Walker and Grant (1996), equilibrium conditions were not found, but significant rate of aggregation of latex particles was observed in the same narrow range of DNA concentrations where mobility flips the sign.

There is a large body of interesting experimental (Rädler et al, 1997; Koltover et al, 1999) and theoretical (Harries et al, 1998; Bruinsma, 1998) work on phase diagrams and overcharging of lamellar cationic lipid-DNA self-assembled complexes. The applicability of the phase diagram similar to Fig. 10 to these systems is doubtful. Indeed, Nguyen and Shklovskii (2001d) clarified that the reentrant condensation is entirely due to the significant difference between two relevant energy scales. Specifically, phase diagram Fig. 10 applies if the energy controlling the stability of necklace structures, or, in general, complexes of a single macroion with some Z -ions, is much larger than the binding energy, u , which controls coalescence of these complexes when they form a condensate. When these two energies are comparable, as they seem

to be in the lipid-DNA system, condensate exists even far from isoelectric line. Phase diagram of this kind was sketched by Rädler (2000).

XI. APART FROM CORRELATIONS, DOES ANYTHING ELSE DRIVE CHARGE INVERSION?

However briefly, we completed the review of works on correlation induced charge inversion. It is now time to ask: Are there alternative, correlation-independent, electrostatic mechanisms leading to this phenomenon? Our answer is no, and we argue that correlations-based mechanism is the universal one. To understand this point deeper, we consider below two theories suggested in literature.

Let us start from the approach which we call *metallization*. It was pioneered by Mateescu et al (1999), who considered complexation of a polyelectrolyte with a sphere, and by Joanny (1999), who examined adsorption of flexible polymers on a charged plane. Metallization theory considers adsorbed Z -ions as a continuous medium similar to a metal, while still treating bulk solution as consisting of discrete charges. Why is smearing so much favorable as to cause adsorption of Z -ions to the macroion which is already neutralized or even overcharged?

The answer is that smearing amounts to *complete* neglect of self-energy of adsorbed Z -ions; better to say, it neglects the energy of each Z -ion's electric field in the range of distances between the ion radius a and macroion size $r \gg a$. On the other hand, correlations can be viewed as physical mechanism eliminating *a part* of self-energy of each Z -ion corresponding to the field in the range of distances between correlation hole size R (which plays the role of screening radius of SCL) and macroion size $r \gg R$. In this sense, metallization overestimates the role of correlations and the charge inversion ratio, particularly when $R \gg a$.

To appreciate the difference between correlated and smeared set of Z -ions, it is worth comparing both to the random distribution of the same ions. Correlated configuration is more favorable than random: correlations happen because ions reconfigure themselves non-randomly to gain some energy. Smeared continuum is also more favorable than random configuration of discrete ions, the difference being precisely the self-energy of ions.

Let us illustrate these ideas in the simplest geometry - a sphere with charge $-Q$ and radius r screened by spherical Z -ions of radius $a \ll r$ in the absence of monovalent salt; self-energy of each Z -ion is $\varepsilon_{self} = Z^2 e^2 / 2\epsilon a$. Correlation theory, as we have seen, results in Eq. (13) for this problem. What does the metallization approach predict? It is easy to write down all relevant energies: $E_{met} = Q^{*2} / 2\epsilon r$, which corresponds to the uniformly smeared net charge Q^* ; $E_{rand} = E_{met} + M\varepsilon_{self}$, which is the energy of the sphere with $M = 4\pi r^2 n$ randomly distributed

Z -ions on its surface; and $E_{WC} = E_{rand} + M\varepsilon(n)$, which is the energy of SCL of Z -ions. Here $\varepsilon(n)$ is given by Eq. (8). The last term of E_{WC} is the correlation energy (Landau and Lifshitz, 1977), it is the negative (favorable) contribution due to the difference between correlated and random configurations of Z -ions. As expected, $E_{met} < E_{WC} < E_{rand}$.

To address equilibrium charge inversion, let us now balance the chemical potential of Z -ions at the surface and in the bulk. Apart from translational entropy contribution negligible at high enough concentrations of Z -ions, the bulk chemical potential is equal to the self-energy ε_{self} while at the surface $\mu = \partial E / \partial M$, where E is either E_{met} , or E_{rand} , or E_{WC} . Therefore, depending on the approximation we want to use, the equilibrium condition reads

$$\begin{aligned} \text{metal : } \quad \varepsilon_{self} &= Q_{met}^* \frac{Ze}{\epsilon r} \\ \text{random : } \quad \varepsilon_{self} &= Q_{rand}^* \frac{Ze}{\epsilon r} + \varepsilon_{self} \\ \text{SCL : } \quad \varepsilon_{self} &= Q_{SCL}^* \frac{Ze}{\epsilon r} + \varepsilon_{self} - 1.65 \frac{Z^2 e^2}{\epsilon R}. \quad (21) \end{aligned}$$

Looking at the result starting from the correlation theory, we see that self-energies cancel and $Q_{SCL}^* = 1.65 Z \epsilon r / R$, producing Eq. (13). By contrast, random distribution leads to $Q_{rand}^* = 0$, i.e., charge inversion is impossible without correlations. Finally, metallization approach yields $Q_{met}^* = Z \epsilon r / 2a$. Comparing with result for SCL, metallization approach is off by a numerical factor only when $R \sim 2a$, while it substantially overestimates charge inversion at $R \gg a$. There is, however, one situation where metallization approximation fails even qualitatively: it does not capture the physics of charge inversion oscillations discussed in the previous section.

Concluding discussion of metallization we would like to emphasize the difference between the metallization approach and the Poisson-Boltzmann one. Poisson-Boltzmann approximation effectively smears Z -ions everywhere, both at the macroion surface and in the bulk of solution, while the metallization approach keeps Z -ions of the bulk discrete. Therefore, it is not surprising that the metallization approach somewhat overestimates charge inversion, while there is no charge inversion in Poisson-Boltzmann approximation.

The other theory, put forward by Park et al (1999), views monovalent *counterion release* from Z -ions as the driving force behind charge inversion. We argue that while counterion release is obviously favorable for charge inversion, it is itself driven by correlations. Let us imagine that DNA molecules, along with their Onsager-Manning-condensed small ions, are being adsorbed on the macroion (possibly releasing some of their counterions), and currently the neutralization condition is achieved. Assume further that DNA rods (Z -ions) are distributed

randomly, uncorrelated in both positions and orientations. In this case, next arriving DNA molecule feels no average field, so that it has no reason to release its counterions. The situation is completely different if DNA molecules are correlated on the surface (see Figs. 2 or 7), where locally each molecule is surrounded by a correlation hole - positive stripe of the background charge (Wigner-Seitz cell). The corresponding field, or positive potential of the Wigner-Seitz cell, causes the release of counterions from DNA not only at the neutrality point, but even if the surface overall is overcharged (see the solution of this problem given by Eqs. (19), (20)). In other words, correlation hole, or adjustment of DNA molecules to each other, or image charge, or correlations (all synonyms!) is a necessary condition for *both* counterion release *and* charge inversion. Interestingly, both of them are driven by correlations! These qualitative arguments can be formulated also more quantitatively (Nguyen et al, 2001).

Closing this section we repeat that the underlying physics of charge inversion is always determined by correlations. An explicit treatment of correlations provides a regular and universal description of this phenomenon. Apart from charge inversion, the correlations manifest themselves also in a number of other ways, including metal-like properties of the macroion surface over certain range of length scales and including the release of counterions.

XII. CHARGE INVERSION IN A BROADER PHYSICS CONTEXT

In conclusion, we would like to show that charge inversion studied in this paper has many physical analogies. There are other "charge inverted" systems in physics. Let us start from the hydrogen atom. It is known that it can bind a second electron, forming negative ion H^- with ionization energy approximately $0.05 Ry$ (Massey, 1938). We can consider this effect as the inversion of proton charge. Attraction of the second electron to the neutral atom is due to the Coulomb correlation between electrons: first electron avoids the second one, spending more time on the opposite side of the proton. In other terms one can say that binding is related to polarization of the neutral core.

Negative ions - nuclei overcharged by electrons - exist also for larger atoms. Mean field Thomas-Fermi or Hartree theories fail to explain negative ions (Landau and Lifshitz, 1977). One must include exchange and Coulomb correlation holes to arrive at a satisfactory theory explaining bound state and nonzero ionization energy of a negative ion (Massey, 1938). Thomas-Fermi theory of an atom is an analog of Poisson-Boltzmann theory of electrolytes. It is not surprising that both fail to explain charge inverted states.

Similar considerations apply also for a macroscopic metallic particle. Electrons in such particle have a negative (compare to vacuum) chemical potential or, in other words, positive work function. The work function is known to vanish in the Thomas-Fermi or Hartree approximations (Lang, 1973).

The energy $|\mu_{WC}|$ plays the same role for Z -ions on the insulating macroion surface as the ionization energy of a negative ion or the work function of metallic particle for electrons. Similarly to electrons, charge inversion of a charged insulating macroion by Z -ions can not be obtained in the mean field Poisson-Boltzmann approximation. Only correlations of Z -ions on the surface of the macroion can lead to charge inversion.

Let us now return to Onsager-Manning condensation (Manning, 1969; Sec. II). Kosterlitz and Thouless (1972) discovered a similar threshold phenomenon for generation of free vortexes in two dimensional superfluids or superconductors. They noticed that due to the logarithmic form of attractive interaction, two vortexes of opposite sign decouple only above some critical temperature, T_{KT} . Later, Kosterlitz-Thouless theory was applied to unbinding of dislocations and disclinations in the theory of defect-induced melting of two-dimensional crystals (Nelson and Halperin, 1979; Young, 1979).

In the Kosterlitz-Thouless theory one can identify analog of the short-range correlation contribution to the chemical potential $|\mu_{WC}|$ of Z -ions. This is the energy of creation of the two vortex cores. Similarly to $|\mu_{WC}|$, this energy provides additional binding of vortexes and strongly reduces the concentration of free vortexes at $T > T_{KT}$ (Minnhagen, 1987). In contrast to the Kosterlitz-Thouless theory, the short range contribution $|\mu_{WC}|$ was only recently introduced (Perel and Shklovskii, 1999).

To conclude, the physical picture of screening for the previously overlooked case of strongly interacting ions presents many parallels with other areas of physics, ranging from quantum Hall effect (Sec. VIII) to atomic physics and metals. With vast array of applications, this theory is one of the busy junctions where physics meets chemistry and biology.

ACKNOWLEDGMENTS

We enjoyed collaboration with V. I. Perel, I. Rouzina, and M. Tanaka. We are grateful to V. Bloomfield, E. Braun, R. Bruinsma, A. Dobrynin, P. Dubin, M. Dyakonov, W. Gelbart, S. Girvin, W. Halley, C. Holm, J.-F. Joanny, A. Khokhlov, R. Kjellander, K. Kremer, A. Koulakov, V. Lobaskin, F. Livolant, D. Long, G. Manning, R. Netz, P. Pincus, R. Podgornik, E. Raspaud, M. Rubinstein, J.-L. Sikorav, U. Sivan, M. Voloshin, and J. Widom for useful discussions. We thank Zhifeng Shao

for the permission to use Figs. 2 and 3 and S. Grant for the permission to use Fig. 11. T. T. N. and B. I. S. are supported by NSF DMR-9985785.

REFERENCES

- Andelman, D., and J. F. Joanny, 2000, cond-mat/0011072.
- Aberts, B., D. Bray, J. Lewis, M. Raff, K. Roberts, J. D. Watson, 1994, *Molecular Biology of the Cell*, Galland Publishing, New York.
- Bloomfield, V. A., 1996, *Current Opinion in Structural Biol.*, **6**, 334; 1998, *Biopolymers*, **44**, 269; Ch. 7 at <http://biosci.umn.edu/biophys/BTOL/supramol.html>
- Braun, E., Y. Eichen, U. Sivan, G. Ben-Yoseph, 1998, *Nature*, **391**, n. 6669, 775.
- Bruinsma, R., 1998, *Europ. Phys. J.* **B4**, 75.
- Chapman, D., 1913, *Philos. Mag. Sixth Ser.* **25**, 475.
- Chodanowski, P., and S. Stoll, 2001, *Macromolecules* **34**, 2320.
- Debye, P., and E. Hückel, 1923, *Phys. Zeitsch.* **24**, 185.
- Dobrynin, A. V., A. Deshkovski, and M. Rubinstein, 2001, *Macromolecules* **34**, 3421.
- Efros, A. L., 1988, *Solid State Comm.* **65**, 1281.
- Eisenstein, J. P., L. N. Pfeifer, and K. W. West, 1992, *Phys. Rev. Lett.* **68**, 674.
- Ennis, J., S. Marcelja, and R. Kjellander, 1996, *Electrochim. Acta* **41**, 2115.
- Evans, H. M., A. Ahmad, T. Pfohl, A. Martin, C. R. Safinya, 2001, *Bull. APS* **46**, 391.
- Fang, Y., and J. Yang, 1997, *J. Phys. Chem.* **B101**, 441.
- Felgner, P. L., 1997, *Scientific American* **276**, 102.
- Gelbart, W., R. Bruinsma, P. Pincus, and A. Parsegian, 2000, *Physics Today* **53**, 38.
- De Gennes, P.-G., P. Pincus, R. M. Velasco, F. Brochard, 1976, *J. de Physique (Paris)*, **37**, 1461.
- Golestanian, R., M. Kardar, and T. B. Liverpool, 1999, *Phys. Rev. Lett.* **82**, 4456.
- Golestanian, R., and M. Kardar, 1999, *Rev. Mod. Phys.* **71**, 1233.
- Götting, N., H. Fritz, M. Maier, J. von Stamm, T. Schoofs, and E. Bayer, 1999, *Colloid Polym. Sci.* **277**, 145.
- Gouy, G., 1910, *J. Phys. Radium* **9**, 457.
- Gronbeck-Jensen, N., R. J. Mashl, R. F. Bruinsma, and W. M. Gelbart, 1997, *Phys. Rev. Lett.* **78**, 2477.
- Guldbrand, L. G., Bo Jonsson, H. Innerstrom, and P. Linse, 1984, *J. Chem. Phys.* **80**, 2221.
- Ha, B.-Y., and A. J. Liu, 1998, *Phys. Rev. Lett.* **81**, 1011; 2000, "Physical Chemistry of Polyelectrolytes," ed. T. Radeva, Marcel Dekker (New York); cond-mat/0003162.
- Harries, D., S. May, W. M. Gelbart, A. Ben-Shaul, 1998, *Biophys. J.* **75**, 159.
- Joanny, J.-F., 1999, *Europ. J. Phys. B* **9**, 117.
- Kabanov, V. A., V. P. Evdakov, M. I. Mustafaeiev, and A. D. Antipina, 1976, *Molekulyarnaya Biologia* **11** 52.
- Keren, K., Y. Soen, G. Ben Yoseph, R. Yechieli, E. Braun, U. Sivan, and Y. Talmon, 2001, preprint.
- Kjellander, R., and S. Marcelja, 1985, *Chem. Phys. Lett.* **114**,

- 124(E).
- Koltover, I., T. Salditt, and C. R. Safinya, 1999, *Biophys. J.* **77**, 915.
- Kosterlitz, J. M., and D. J. Thouless, 1972, *J. Phys C* **5**, L124; 1973, *J. Phys C* **6**, 1181.
- Kravchenko, S. V., D. A. Rinberg, S. G. Semenchinsky, and V. Pudalov, 1990, *Phys. Rev. B* **42**, 3741.
- Landau, L. D., and E. M. Lifshitz, 1977, *Statistical Physics, Part 1* (Pergamon Press, Oxford), Ch. VII.
- Landau, L. D., and E. M. Lifshitz, 1980, *Quantum Mechanics (nonrelativistic theory)* (Pergamon Press, Oxford), Ch. X.
- Lang, N. D., 1973, *Solid state physics*, Edited by H. Ehrenreich, F. Seitz, and D. Turnbull, (Academic Press, New York), Vol. 28.
- Lau, A. W. C., P. A. Pincus, 1998, *Phys. Rev. Lett* **81**, 1338.
- Levin, Y., J. J. Arenzon, and J. F. Stilck, 1999, *Phys. Rev. Lett.* **83**, 2680.
- Linse, P., and V. Lobaskin, 1998, *Phys. Rev. Lett.*, **83**, 4208.
- Luger, K., A. Mader, R. Richmond, D. Sargent, T. Richmond, 1997, *Nature*, **389**, 251. For pictures visit, e.g. <http://info.bio.cmu.edu/Courses/03438/Nsome/1AOI.htm>
- Manning, G.S., 1969, *J. Chem. Phys.* **51**, 924.
- Massey, H.S.W., 1938, *Negative Ions*, Cambridge University Press.
- Mateescu, E. M., C. Jepperseni, and P. Pincus, 1999, *Europhys. Lett.* **46**, 454.
- Messina, R., C. Holm, and K. Kremer, 2000, *Phys. Rev. Lett.* **85**, 872; 2000, *Europhys. Lett.* **51**, 461.
- Minnhagen, P., 1987, *Rev. Mod. Phys* **59**, 1001.
- Moreira, A. G., R. R. Netz, 2000a, *Europhys. Lett.* **52**, 705.
- Moreira, A. G., R. R. Netz, 2000b, *cond-mat/0009377*.
- Mou, J., D. M. Czajkowsky, Y. Zhang, and Z. Shao, 1995, *FEBS Letters* **371**, 279.
- Nelson, D. R., and B. I. Halperin, 1979, *Phys. Rev. B* **19**, 2457.
- Netz, R. R., and J. F. Joanny, 1999a, *Macromolecules*, **32**, 9013.
- Netz, R. R., J. F. Joanny, 1999b, *Macromolecules*, **32**, 9026.
- Nguyen, T. T., A. Yu. Grosberg, and B. I. Shklovskii, 2000a, *Phys. Rev. Lett.* **85**, 1568.
- Nguyen, T. T., A. Yu. Grosberg, and B. I. Shklovskii, 2000b, *J. Chem. Phys.* **113**, 1110.
- Nguyen, T. T., I. Rouzina, B. I. Shklovskii, 2000, *J. Chem. Phys.* **112**, 2562.
- Nguyen, T. T., A. Yu. Grosberg, and B. I. Shklovskii, 2001, in *Electrostatics effects in Biophysics and soft matter*, C. Holm, P. Kekicheff, R. Podgornik eds, Kluwer; *condmat/0101103*.
- Nguyen, T. T., and B. I. Shklovskii, 2001a, *Physica A* **293**, 324.
- Nguyen, T. T., and B. I. Shklovskii, 2001b, *J. Chem. Phys.* **114**, 5905.
- Nguyen, T. T., and B. I. Shklovskii, 2001c, *Phys. Rev. E*; *cond-mat/0103208*.
- Nguyen, T. T., and B. I. Shklovskii, 2001d, *cond-mat/0105078*.
- Onsager, L., 1967, private communication to G. Manning.
- Oosawa, F., 1968, *Biopolymers* **6**, 134.
- Pan, J., D. Thirumalai, S. Woodson, 1999, *Proc. Natl. Acad. Sci.*, **96**, 6149.
- Park, S. Y., R. F. Bruinsma, and W. M. Gelbart, 1999, *Europhys. Lett.* **46**, 493.
- Pelta, J., D. Durand, J. Doucet, and F. Livolant, 1996, *Biophys. J.* **71**, 48.
- Pelta, J., F. Livolant, and J.-L. Sikorav, 1996, *J. Biol. Chem.* **271**, 5656.
- Perel, V. I., and B. I. Shklovskii, 1999, *Physica A* **274**, 446.
- Podgornik, R., and V. A. Parsegian, 1998, *Phys. Rev. Lett.* **80**, 1560.
- Potemkin, I. I., K. B. Zeldovich, A. R. Khokhlov, 2000, *Polymer Science, Ser. C*, **42**, 154.
- Rädler, J. O., I. Koltover, T. Salditt, and C. R. Safinya, 1997, *Science*, **275**, 810.
- Rädler, J. O., 2000, in *Electrostatics effects in Biophysics and soft matter*, C. Holm, P. Kekicheff, R. Podgornik eds, Kluwer.
- Raspaud, E., M. Olvera de la Cruz, J.-L. Sikorav, and F. Livolant, 1998, *Biophys. J.* **74**, 381.
- Raspaud, E., I. Chaperon, A. Leforestier, and F. Livolant, 1999, *Biophys. J.* **77**, 1547.
- Rau, D. C., and A. V. Parsegian, 1992, *Biophys. J.* **61**, 246.
- Rouzina, I., and V. A. Bloomfield, 1996, *J. Phys. Chem.* **100**, 9977.
- Saminathan, M., T. Antony, A. Shirahata, L. Sigal, T. Thomas, and T. J. Thomas, 1999, *Biochemistry* **38**, 3821.
- Sens, P., and E. Gurovitch, 1999, *Phys. Rev. Lett.* **82**, 339.
- Shao, Z., 1999, *News in Physiological Sciences*, **14**, 142.
- Shklovskii, B. I., 1999a, *Phys. Rev. Lett.* **82**, 3268.
- Shklovskii, B. I., 1999b, *Phys. Rev. E* **60**, 5802.
- Tanaka, M., and A. Yu. Grosberg, 2001, *J. Chem. Phys.* **114**, ???; *cond-mat/0102209*.
- Tanaka, M., A. Yu. Grosberg, 2001, unpublished result.
- Terao, T., and T. Nakayama, 2001, *Phys. Rev. E* **63**, 041401.
- Totsuji, H., 1978, *Phys. Rev. A* **17**, 399.
- Walker, H. W., and S. B. Grant, 1996, *Colloids and Surfaces A*, **119**, 229.
- Wallin, T., P. Linse, 1996, *J. Phys. Chem.* **100**, 17873; 1997 *ibid* **101**, 5506.
- Wang, Y., K. Kimura, Q. Huang, P. L. Dubin, and W. Jaeger, 1999, *Macromolecules* **32**, 7128.
- Woodson, S., 2000, *Nature Structural Biology*, **7**, 349.
- Xia, J., and P. L. Dubin, 1994, *Macromolecular complexes in Chemistry and Biology* P. L. Dubin et al. eds. (Springer-Verlag, Berlin).
- Young, A., 1979, *Phys. Rev. B* **19**, 1855.
- Zimm, B., and M. Le Bret, 1983, *J. Biomol. Struct. and Dyn.* **1**, 461.